BRIEF DEFINITIVE REPORT

Expression of factor V by resident macrophages boosts host defense in the peritoneal cavity

Nan Zhang[1] , Rafael S. Czepielewski[1] , Nicholas N. Jarjour[1], Emma C. Erlich[1], Ekaterina Esaulova[1] , Brian T. Saunders[1] , Steven P. Grover[3], Audrey C. Cleuren[4] , George J. Broze[2], Brian T. Edelson[1] , Nigel Mackman[3], Bernd H. Zinselmeyer[1], and Gwendalyn J. Randolph[1]

Macrophages resident in different organs express distinct genes, but understanding how this diversity fits into tissue-specific features is limited. Here, we show that selective expression of coagulation factor V (FV) by resident peritoneal macrophages in mice promotes bacterial clearance in the peritoneal cavity and serves to facilitate the well-known but poorly understood "macrophage disappearance reaction." Intravital imaging revealed that resident macrophages were nonadherent in peritoneal fluid during homeostasis. Bacterial entry into the peritoneum acutely induced macrophage adherence and associated bacterial phagocytosis. However, optimal control of bacterial expansion in the peritoneum also required expression of FV by the macrophages to form local clots that effectively brought macrophages and bacteria in proximity and out of the fluid phase. Thus, acute cellular adhesion and resident macrophage–induced coagulation operate independently and cooperatively to meet the challenges of a unique, open tissue environment. These events collectively account for the macrophage disappearance reaction in the peritoneal cavity.

Introduction

Our understanding of the biology of tissue-resident macrophages has evolved greatly in the past decade. Resident macrophages in most organs arrive during embryogenesis, maintaining themselves for long periods via local proliferation (Ginhoux and Guilliams, 2016). These resident macrophages express specialized sets of genes that are distinct between different organs (Gautier et al., 2012). Even when monocytes are recruited to these organs during inflammation, the inflammatory macrophages they become are reticent to take up the specialized resident phenotype, if they do at all (Gautier et al., 2013; Guilliams and Scott, 2017; Misharin et al., 2017). It is assumed that specialized genes expressed by particular resident macrophages encode products tailored to the specific physiological needs or constraints of that tissue, but illustration of direct links often remain unexplored. Transcription factors that regulate specialized macrophage gene sets in different organs have, however, been identified. One such transcription factor is Gata6, which selectively governs the life cycle of murine resident peritoneal macrophages, often called large peritoneal macrophages (LPMs; Gautier et al., 2012, 2014; Okabe and Medzhitov, 2014; Rosas et al., 2014). In this study, we focused on understanding how the transcriptional profile of resident peritoneal macrophages could be linked to the specialized function of these cells.

Results and discussion

A prominent example of tissue-restricted gene expression in macrophages is the selective detection in LPMs of mRNA for coagulation factors, including factor V (FV; *F5*), FVII (*F7*), and FX (*F10*; Fig. 1 A). The latter two factors were also expressed by lung macrophages, whereas FV was unique to peritoneal macrophages. Activated FV is a key cofactor in the common pathway for activated FX, forming the prothrombinase complex that, during coagulation, converts prothrombin to thrombin that in turn converts fibrinogen to fibrin to form clots. Indeed, the coagulation pathway was among top pathways selectively enriched in LPMs (Gautier et al., 2012). The unique expression of FV, in particular, among tissue-resident macrophages caused us to consider the possibility that coagulation may have a key role in peritoneal macrophage function. The expression of FVII, important for initiating the extrinsic pathway of coagulation in complex with tissue factor (TF; *F3*) that is acutely induced after tissue damage, led us to consider this pathway of coagulation in particular.

A classic response to inflammation exhibited by LPMs is known as the "macrophage disappearance reaction" (MDR), first described decades ago (Nelson, 1963). In this reaction, LPMs become irretrievable from lavage just hours after introduction of

[1]Department of Pathology and Immunology, Washington University School of Medicine, St. Louis, MO; [2]Department of Medicine, Washington University School of Medicine, St. Louis, MO; [3]Department of Medicine, University of North Carolina at Chapel Hill, Chapel Hill, NC; [4]Life Sciences Institute, University of Michigan, Ann Arbor, MI.

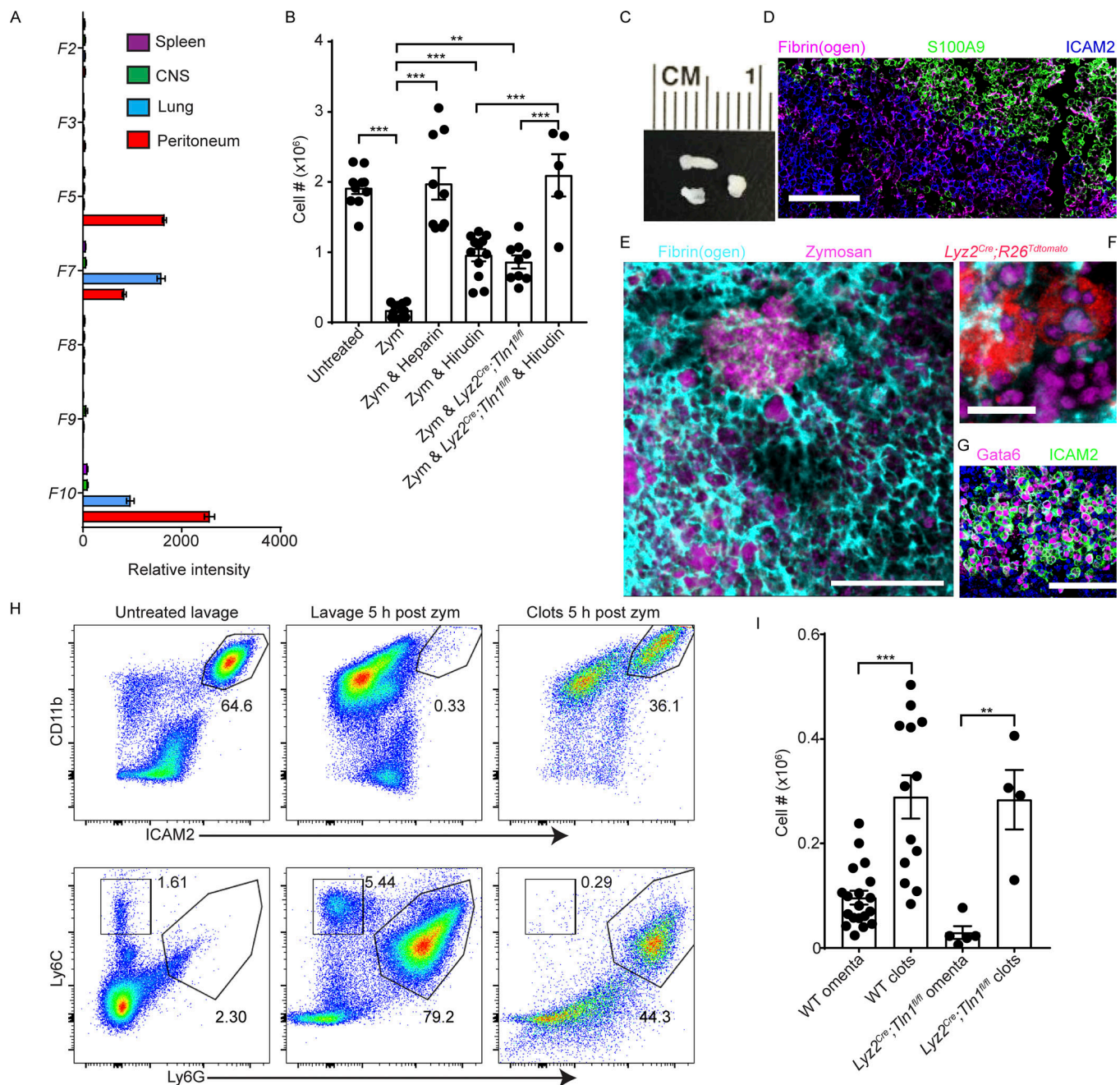Correspondence to Gwendalyn J. Randolph: gjrandolph@wustl.edu.

Figure 1. Coagulation and adhesion additively cooperate to account for the MDR in response to inflammation. (A) Gene array analysis (from ImmGen; n = 3 separate pools) of classical coagulation factors in major tissue resident macrophages, including those from the spleen, central nervous system (CNS), lung, and peritoneum. **(B)** Quantification of LPMs in peritoneal lavage 3 h after zymosan injection i.p. when clotting and/or adhesion was inhibited. **(C)** Aggregates retrieved from the peritoneum 5 h after zymosan injection. **(D–G)** Immunofluorescence staining of the aggregates for fibrin(ogen) and macrophage markers. D and G are stained frozen sections of the clots; E and F are whole-mount preparations. Scale bars represent 100 μm (D and G), 50 μm (E), and 10 μm (F). **(H)** Flow cytometry on peritoneal exudate cells from untreated mice (left), 3 h after zymosan i.p. (middle), and clots 3 h after zymosan i.p. (right). **(I)** Quantification of LPMs 3 h after zymosan injection in clots and omenta in WT and Lyz2Cre;Tln1fl/fl mice. One-way ANOVA was used to test statistical significance. Symbols represent individual mice studied. Error bars represent ± SEM. All experiments were repeated at least two or three times. **, P < 0.01; ***, P < 0.001.

inflammatory stimuli like the bacillus Calmette-Guerin vaccine, lipopolysaccharide, zymosan, or thioglycollate (Nelson, 1963; Barth et al., 1995; Davies et al., 2013; Gautier et al., 2013; Meza-Perez and Randall, 2017). Repopulation of resident macrophages is slow following the MDR. LPMs are not always restored after

inflammation otherwise appears to have resolved (Gautier et al., 2013). In the 1960s, Nelson proposed a role for coagulation in the MDR, because he could fully reverse it by administering heparin, which can block coagulation or adhesion; MDR was also reversed to an appreciable but lesser extent by warfarin, which

Table 1. **Peritoneal fluid volume, peritoneal cell density, and total cell and macrophage numbers in 6-wk-old C57BL/6J mice (comparison of lavage and collection of undiluted fluid)**

	Volume (µl ± SEM)	Cell density (×10⁴/µl ± SEM)	Total cells (×10⁶ ± SEM)	Gata6⁺ resident macrophages (×10⁶ ± SEM)
Peritoneal fluid	52.14 ± 4.02 (7)	6.50 ± 0.85 (6)	3.26 ± 0.27 (6)	1.73 ± 0.11 (6)
Lavage	N/A	N/A	3.20 ± 0.15 (12)	1.81 ± 0 09 (12)

Numbers in parentheses indicate the numbers of mice used. N/A, not applicable.

would more specifically target coagulation (Nelson, 1963). In the ensuing years, with recognition that fibrin(ogen) participates in adhesion, the view developed that coagulation factors support macrophage disappearance by promoting adhesion and migration (Szaba and Smiley, 2002) to locations like the omentum during the MDR (Meza-Perez and Randall, 2017). Thus, a classical role for coagulation in peritoneal host defense was largely overlooked. Our intravital imaging of the peritoneal cavity through an intact abdominal wall indicated that a distinct feature of LPMs, relative to resident macrophages in other organs, is that they are free floating in peritoneal fluid (Video 1). LPMs only adhered to the walls of the peritoneal cavity covering visceral organs after inflammatory stimuli (heat-killed bacteria) were introduced (Video 1). Cell density in peritoneal fluid was high, at ~6.5 × 10⁴/µl (Table 1), ~20× the concentration of leukocytes in blood (Mouse Phenome Database; The Jackson Laboratory).

Given this literature and the striking expression of coagulation factors in LPMs, we wondered whether coagulation might drive important processes in the peritoneum. First, we confirmed that heparin fully reversed the MDR induced by 1 mg zymosan i.p. (Fig. 1 B). The very selective inhibitor of thrombin hirudin partially (~50%) inhibited MDR (Fig. 1 B), reminiscent of the effect of warfarin relative to heparin (Nelson, 1963). Heparin has both anticoagulant and anti-adhesive activity (Woods et al., 1986), and this may explain why it is more effective at inhibiting MDR compared with either warfarin or hirudin.

To directly address the role of integrin–mediated adhesion in MDR, in the same experiments we employed *Lyz2^Cre;Tln1^fl/fl* mice (Fig. 1 B) to prevent en bloc activation of integrins through loss of the integrin activation adaptor talin-1 (*Tln1*) in lysozyme-expressing cells (Yago et al., 2015), which includes LPMs and other myeloid cells like neutrophils (Faust et al., 2000). The absence of integrin signaling also partially inhibited MDR, similar to the inhibition achieved with hirudin alone (~50%). However, rather than being redundant, the combination of hirudin and genetic loss of *Tln1* had additive effects, such that when the two interventions were combined, MDR was fully reversed, mirroring heparin (Fig. 1 B). In addition, because neutrophil infiltration almost always correlates with MDR after zymosan injection, we tested the hypothesis that infiltrated neutrophils cause MDR. Results from depleting neutrophils with

anti-Ly6G mAb (Fig. S1 A) demonstrated the neutrophils were dispensable as a cause for MDR (Fig. S1 B). Furthermore, neutrophil recruitment was unaffected by *Tln1* deficiency in this model (Fig. S1, C and D), which is consistent with previous report (Lim and Su, 2018). We conclude that neutrophil infiltration does not play a role in MDR in this model. However, integrin–mediated adhesion is relevant to MDR, but such adhesion cannot account for a distinct, prominent role of the coagulation cascade in affecting macrophage removal.

A close physical examination of the peritoneal cavity after MDR revealed millimeter-sized aggregates within the peritoneal cavity 3–5 h after i.p. injection of zymosan (Fig. 1 C). These aggregates stained positively for fibrin(ogen) (Fig. 1, D–F), indicating that they were clots, with such staining most easily appreciated in whole-mount preparations where strands of fibrin were observed between clumps of zymosan particles and cells (Fig. 1, E and F). Clots were also enriched in LPMs identified by coexpression of Gata6 and ICAM2 (Fig. 1 G), but very few peritoneal B cells were incorporated into the clots (Fig. S1 E), despite that peritoneal B cells are almost as abundant as macrophages in the steady state peritoneal fluid. Some macrophages in clots were loaded with zymosan particles, but other zymosan particles appeared outside of cells (Fig. 1, E and F), suggesting that clots were efficient at entrapping debris not yet phagocytized. Clots also incorporated S100A9⁺ neutrophils, which are known to be rapidly recruited to the peritoneum after zymosan is injected i.p. (Fig. 1 D). Flow cytometry confirmed enrichment of LPMs in the clots, while they were largely absent in the lavage 3 h after i.p. zymosan (Fig. 1 H). Approximately three times more LPMs were recovered in clots compared with the omentum (Fig. 1 I), indicating that clots are prominent sites for macrophage "disappearance" in response to inflammatory triggers. Consistent with the integrin independence of macrophage inclusion in clots, macrophage recovery from clots was unaffected by *Tln1* deficiency (Fig. 1 I), whereas recovery from the omentum trended downward, consistent with a role for adhesion in retaining macrophages in the omentum.

Work beginning in the 1980s revealed that LPMs produce FV in culture (Osterud et al., 1981), including production of a functional prothrombinase complex (activated FV/activated FX; Pejler et al., 2000) long before it was recognized that *F5* mRNA expression was selective to LPMs. Although the liver is a known source of FV, expression of FV by LPMs led us to hypothesize these macrophages maintain FV levels in peritoneal fluid in the steady state. We thus analyzed FV activity in peritoneal fluid using a one-stage clotting assay. In WT C57BL/6J mice, FV activity in peritoneal interstitial fluid was ~13% of that in plasma (Fig. 2 A), consistent with the documented poor entry of plasma proteins as large as FV (a ~300-kD protein) into interstitial fluid of molecules (Yang et al., 1998; Michel et al., 2015). Peritoneal fluid was thus analyzed from *F5^−/−;AlbF5Tg* mice, engineered such that the liver sustains expression of FV from the albumin promoter but all other tissues, including LPMs, lack FV (Sun et al., 2003). These mice displayed a ~75% reduction in FV activity compared with WT peritoneal fluid (Fig. 2 A), raising the possibility that the major source of FV in the peritoneal fluid was not the liver.
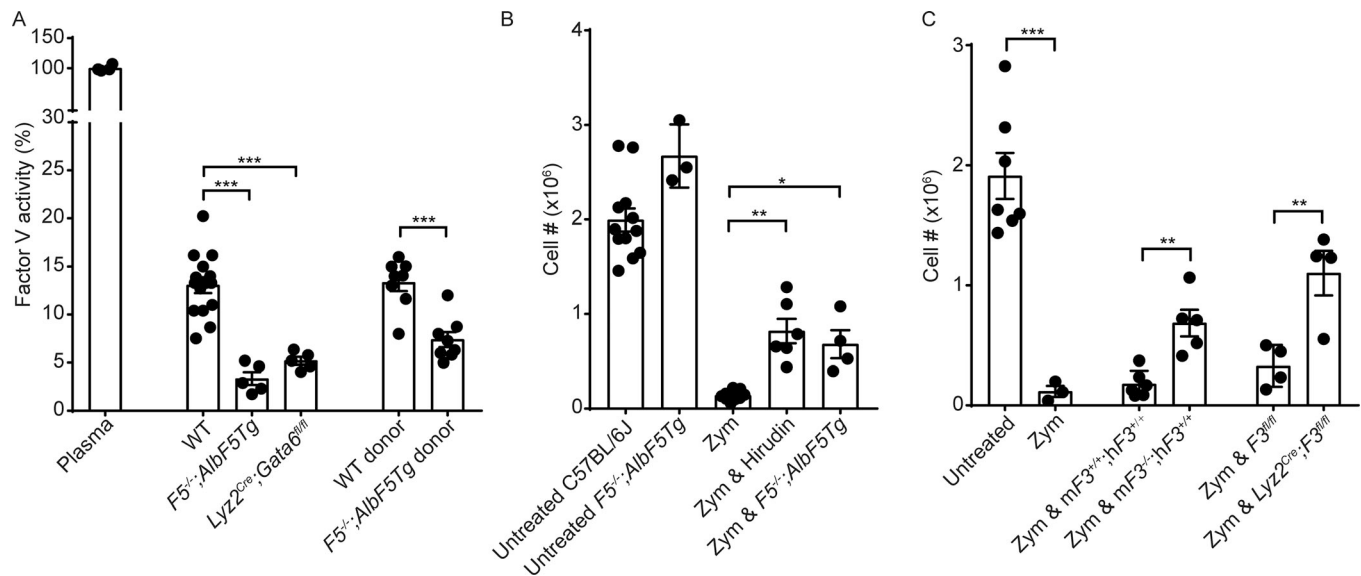
Figure 2. FV and TF from resident peritoneal macrophages are responsible for peritoneal fluid clotting. (A) Quantification of FV activity in plasma or peritoneal fluid of various genotypes of mice or after bone marrow transplant of indicated donor genotypes into irradiated WT recipients (last bars on the right). Zym, zymosan. **(B)** Quantification of LPMs 3 h after zymosan injection. **(C)** Quantification of LPMs 3 h after zymosan injection. One-way ANOVA was used to test statistical significance, except for the bone marrow chimera result in B and the $hF^{+/+}$ groups and $F3^{fl/fl}$ groups in C, which used a two-tailed t test. Symbols represent individual mice studied. Error bars represent ± SEM. All experiments were repeated at least two or three times. *, P < 0.05; **, P < 0.01; ***, P < 0.001.

Demonstrating that a major local source of FV was LPMs, FV activity in peritoneal fluid of the $Lyz2^{Cre};Gata6^{fl/fl}$ mouse, which lack most LPMs (Gautier et al., 2014; Okabe and Medzhitov, 2014; Rosas et al., 2014), mirrored the very low level in $F5^{-/-};AlbF5Tg$ mice (Fig. 2 A). LPMs are the only immune cell in the mouse that expresses Gata6 (Gautier et al., 2014). Thus, while $Lyz2^{Cre}$ is not completely selective to LPMs, $Lyz2^{Cre};Gata6^{fl/fl}$ mice exhibit a highly selective defect in LPMs (Gautier et al., 2014). As an additional evaluation, we performed bone marrow transplantation using WT or $F5^{-/-};AlbF5Tg$ marrow as donors for irradiated WT recipients that would have normal liver FV. With 80–85% reconstitution of resident peritoneal macrophages with donor marrow (data not shown), mice receiving $F5^{-/-};AlbF5Tg$ marrow showed significantly lower FV activity in peritoneal fluid than mice receiving WT marrow (Fig. 2 A, bars on right).

We then hypothesized that this LPM–derived FV is crucial to promote early local clotting in the peritoneal fluid. Indeed, the zymosan-induced MDR in $F5^{-/-};AlbF5Tg$ mice reduced the MDR to a similar level as the hirudin-treated group (Fig. 2 B), suggesting that FV from LPMs is critical for the peritoneal clotting in this model. Thus, we conclude that LPMs produce FV in the steady state that in turn promotes clotting of local interstitial fluid during the MDR (Sun et al., 2003).

In the extrinsic coagulation cascade, TF (FIII; F3) initiates clotting and has in other systems been demonstrated to be rapidly expressed by macrophages upon activation. We observed rescue of MDR in response to zymosan-injected i.p. in mice deficient for murine TF that express very low human TF levels (h$F3$; ~1%; m$F^{-/-}$;Lowh$F3^{+/+}$), in contrast to control mice with normal TF levels (m$F^{+/+}$;Lowh$F3^{+/+}$; Fig. 2 C). The 1% of normal TF levels in the h$F3$ transgenic mouse can restore viability of the line but has a markedly impaired capacity to initiate

extrinsic coagulation (Parry et al., 1998), while their control counterparts from a sister line expressing the human transgene as well as murine F3 exhibited a complete MDR in response to zymosan (Fig. 2 C). Likewise, the MDR was partially suppressed in $Lyz2^{Cre};F3^{fl/fl}$ mice (Pawlinski et al., 2010) compared with $F3^{fl/fl}$ control mice (Fig. 2 C). Even though $F3$ mRNA is not detectable in resting LPMs (Fig. 1 A), TF can be rapidly (within 1 h) up-regulated on the LPM surface and is capable of initiating clotting in vitro (data not shown). Thus, it is likely that LPMs quickly generate enough TF to initiate the extrinsic coagulation cascade during the MDR.

Finally, we wondered whether clotting of interstitial fluid had a critical functional role. While clotting of interstitial fluid would seem irrelevant to hemostasis, we wondered if interstitial clotting might serve to entrap both free-floating macrophages and microbes that invade the peritoneum. Indeed, a previous study revealed that a single dose of heparin or hirudin caused increased mortality after mice were subjected to cecal-ligation puncture (Echtenacher et al., 2001), although the role of local cells and factors remained unclear. To investigate whether LPM-dependent local peritoneal coagulation controlled peritoneal infection, we measured the thrombin–antithrombin complex (TAT), the standard assay to track occurrence of coagulation, in the peritoneal fluid and plasma over time after i.p. infection with live $E. coli$ (Fig. 3 A), normalizing the data as a percentage of maximal TAT in the serum from exogenously clotted plasma. Both peritoneal and blood TAT were below detection in the steady state using the assay. However, peritoneal but not blood TAT complex was detected within 2 h of infection, lasting for at least 6 h (Fig. 3 A). In tamoxifen-treated $CsfIr^{MeriCreMer};Gata6^{fl/fl}$ or $Lyz2^{Cre};Gata6^{fl/fl}$ mice, which exhibit selectively and greatly reduced LPMs (Gautier et al., 2014), TAT was an average of 48%
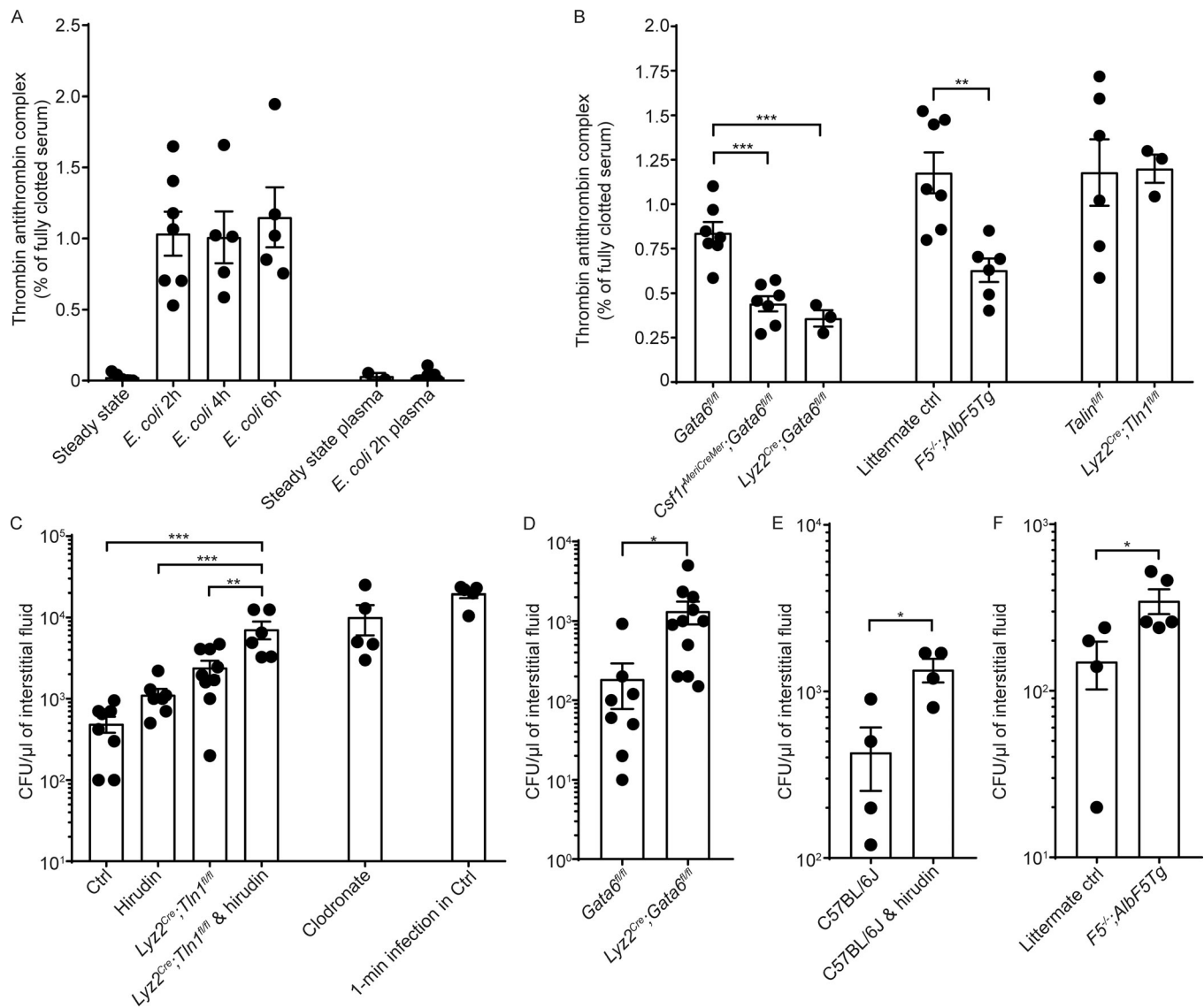
Figure 3. **Macrophage adhesion and macrophage-driven clotting cooperatively promote peritoneal bacterial clearance. (A)** Quantification of TAT complex in peritoneal fluid and plasma in the steady state or after *E. coli* infection. **(B)** Quantification of TAT complex in peritoneal fluid 4 h after *E. coli* infection. Ctrl, control. **(C)** CFUs per microliter peritoneal fluid from untreated, hirudin-treated WT, *Lyz2^Cre^;Talin^fl/fl^* mice, hirudin-treated *Lyz2^Cre^;Talin^fl/fl^* mice, and clodronate liposome-treated mice 4 h after *E. coli* infection. **(D)** CFUs per microliter peritoneal fluid from *Gata6^fl/fl^* and *Lyz2^Cre^;Gata6^fl/fl^* mice 4 h after *E. coli* infection. **(E)** CFUs per microliter peritoneal fluid from C57BL/6J treated with or without hirudin 4 h after *E. coli* infection. **(F)** CFUs per microliter peritoneal fluid from control and *F5^−/−^;AlbF5Tg* mice 4 h after *E. coli* infection. One-way ANOVA was used to test statistical significance, except for C, D, and F and the *F5^−/−^;AlbF5Tg* groups in B, which were examined by a two-tailed *t* test. Symbols represent individual mice studied. Error bars represent ± SEM. All experiments were repeated at least two or three times. *, $P < 0.05$; **, $P < 0.01$; ***, $P < 0.001$.

and 57% lower, respectively, than in control mice upon infection. Furthermore, *F5^−/−^;AlbF5Tg* mice showed comparably reduced peritoneal TAT after infection (Fig. 3 B). As expected, *Tln1* deficiency in macrophages did not affect TAT levels (Fig. 3 B), and neither did neutrophil depletion (data not shown). These data indicate that Gata6+ resident macrophages contribute substantially to peritoneal coagulation in an FV-dependent manner early after infection. Even though it would be anticipated that the infectious state would increase vascular permeability and allow for increased influx of plasma–derived proteins, the data indicate that any role for permeability in bringing in plasma FV in the few hours after infection is not sufficient to raise TAT to levels observed in mice that can generate local FV. Nonetheless,

an increase in permeability might account for why TAT levels are not as low as the basal level of FV observed in resting mice.

We next investigated the functional impact of MDR on local bacterial clearance during a 4-h period following infection. Inhibition of both clotting and macrophage adhesion to collectively block the MDR dramatically increased CFUs in the peritoneal fluid compared with untreated mice, clotting-inhibited mice, or adhesion-blocked mice (Fig. 3 C), strongly suggesting that both clotting and adhesion are required for optimal bacterial clearance. By examining bacterial numbers that we could retrieve from the peritoneal cavity 1 min after their installation (Fig. 3 C, right column) and comparing with all data obtained at 4 h, it was clear that all CFUs recovered at 4 h were reduced from the

numbers instilled. Thus, CFUs assessed at 4 h served primarily to assess how efficiently bacteria were cleared rather than to assess bacterial growth. In the absence of any interference to the MDR, an average of 98% of bacteria were cleared in 4 h compared with the number of CFUs retrieved at 1 min. When macrophages had earlier been depleted from the peritoneal cavity with clodronate-loaded liposomes without affecting blood monocytes, as per previous protocol (Wang and Kubes, 2016), clearance of bacteria was much less efficient, at only 49%, indicating the pivotal role of local macrophages in bacterial removal. With use of hirudin alone or loss of *Tln1* alone, clearance of bacteria averaged 93% and 86%, respectively. Remarkably, when both coagulation and adhesion were inhibited, clearance at 4 h decreased to an average of 64%, approaching the impact that complete macrophage depletion achieved (Fig. 3 C). Thus, these data strongly suggest that both coagulation and adhesion optimize bacterial clearance from the peritoneal cavity.

We then wondered if LPMs or LPM-dependent clotting played a significant role in accounting for the overall role played by macrophages in bacterial clearance as revealed from the use of the clodronate-loaded liposomes. Mice genetically lacking the majority of LPMs (*Lyz2^Cre;Gata6^fl/fl*) showed CFUs approximately seven times higher than those of control mice (Fig. 3 D). Deficiency in hematopoietic FV (*F5^−/−;AlbF5Tg*) also reduced CFU by two- to threefold (Fig. 3 F), confirming that local FV accounted for the role of coagulation in local bacterial clearance. Intravital imaging of clots ex vivo showed *Escherichia coli* within lysozyme+ cells at the time of imaging and other motile bacteria not yet engulfed by phagocytes but nonetheless trapped within the clot (Video 2).

Lastly, we investigated whether the local control of bacteria by the MDR or clotting had any impact on bacterial dissemination from the peritoneal cavity to the blood and ultimately the spleen. Dissemination is a complex evaluation because there can be roles for leukocytes or coagulation beyond the peritoneum within the vasculature itself. The most ideal experimental scenario would be one in which the tools applied to the question of dissemination from the peritoneum would have neutral effects on CFU in the spleen after *E. coli* administration in the blood so that the effects from the peritoneum could be more selectively evaluated. Thus, we first evaluated whether the tools we used in the peritoneal cavity that regulate adhesion, including the *Lyz2^Cre;Tln1^fl/fl* mouse strain and heparin, altered CFUs in the spleen after i.v. delivery, as any effects in this arm of the experiment could confound interpretation of dissemination from the peritoneum. Indeed, and surprisingly, *Lyz2^Cre;Tln1^fl/fl* mice displayed fewer CFUs in the spleen after *E. coli* delivery i.v. (Fig. 4 A). This protective effect of *Tln1* deficiency in blood myeloid cells might be expected to offset our predicted increase in dissemination of *E. coli* from the peritoneum. By contrast, heparin administered i.p. did not show any statistically significant effect on CFU in the spleen after i.v. administration of *E. coli* (Fig. 4 B). *F5^−/−;AlbF5Tg* mice and hirudin administered i.p. also had neutral effects on *E. coli* CFUs in the spleen when *E. coli* was administered i.v. (Fig. 4, B and C). With respect to adhesion, because *Tln1* deficiency was not neutral in the blood–spleen compartment (Fig. 4 A), we sought to block macrophage adhesion using antibodies rather than *Tln1* deficiency. Combined

blockade of β1 and β2 integrins would be expected to interfere with adhesion of peritoneal macrophages to mesothelial walls (Bellingan et al., 2002; Cao et al., 2005) and, fortunately, neutralizing mAbs to these molecules had a neutral impact on *E. coli* CFUs in the spleen when *E. coli* was administered to blood (Fig. 4 B). These data thus indicate that the most optimal tools in hand to next evaluate the impact of macrophage–mediated coagulation and adhesion on *E. coli* dissemination from the peritoneum were *F5^−/−;AlbF5Tg* mice, heparin, or hirudin to block coagulation and combined anti-β1 and -β2 mAbs to block adhesion.

When we next instilled *E. coli* into the peritoneal cavity to study its dissemination, mice with a complete loss of MDR through the use of heparin exhibited markedly elevated CFUs in the spleen at 16 h after *E. coli* i.p. instillation (Fig. 4 D). Furthermore, hematopoietic FV-deficient (*F5^−/−;AlbF5Tg*) mice treated with blocking antibodies against both β1 and β2 integrins showed significantly increased CFUs in the spleen when *E. coli* were administered i.p. (Fig. 4 E). Mice treated with both hirudin and blocking antibodies against β1 and β2 integrins showed significantly increased bacterial burden in the spleen at 16 h after *E. coli* i.p. instillation compared with those treated with anti-β1 and β2 mAbs alone (Fig. 4 F), demonstrating that clotting indeed impacted bacterial dissemination, beyond the impact of impaired adhesion. *Tln1* deficiency in myeloid cells, combined with hirudin, did not affect dissemination (Fig. 4 G), but this is likely due to the conflicting roles of *Tln1* deficiency in the peritoneum (Fig. 1 B) versus the blood (Fig. 4 A). Together, these data strongly suggest that the two processes that cooperatively and nonredundantly account for the MDR, coagulation and adhesion, also cooperatively and nonredundantly function to optimize bacterial clearance from the peritoneal cavity, which is essential to contain dissemination.

These studies, in summary, illustrate how specialized gene expression in a particular macrophage is intimately tied to the unique characteristics and physiology of the organ. Specifically, to support high-quality host defense in the capture of microorganisms that might gain access to the peritoneal cavity through the digestive tract, resident peritoneal macrophages constitutively produce FV, along with other clotting factors. This production makes up for the minimal access that liver–derived FV has to the peritoneum. Expression of FV allows macrophages to generate clots that trap microorganisms even before they have a chance to be phagocytosed. This form of host defense is especially relevant in a fast-flowing environment of fluid that comprises a challenging space for efficient phagocytosis. While the clots collect microorganisms in large numbers, additional macrophages adhering within the omentum and upon visceral organ surfaces undoubtedly promote capture of organisms that avoided entrapment in clots. These two mechanisms collectively account for the vast majority of macrophage disappearance in the context of peritoneal inflammation, and our data indicate that both arms of the MDR, adhesion and coagulation, are required for optimal host defense. Finally, in many clinical scenarios, therapeutic agents are used to limit coagulation to minimize its occurrence in blood. The present work, however, illustrates that in the particular tissue microenvironment of the peritoneum,
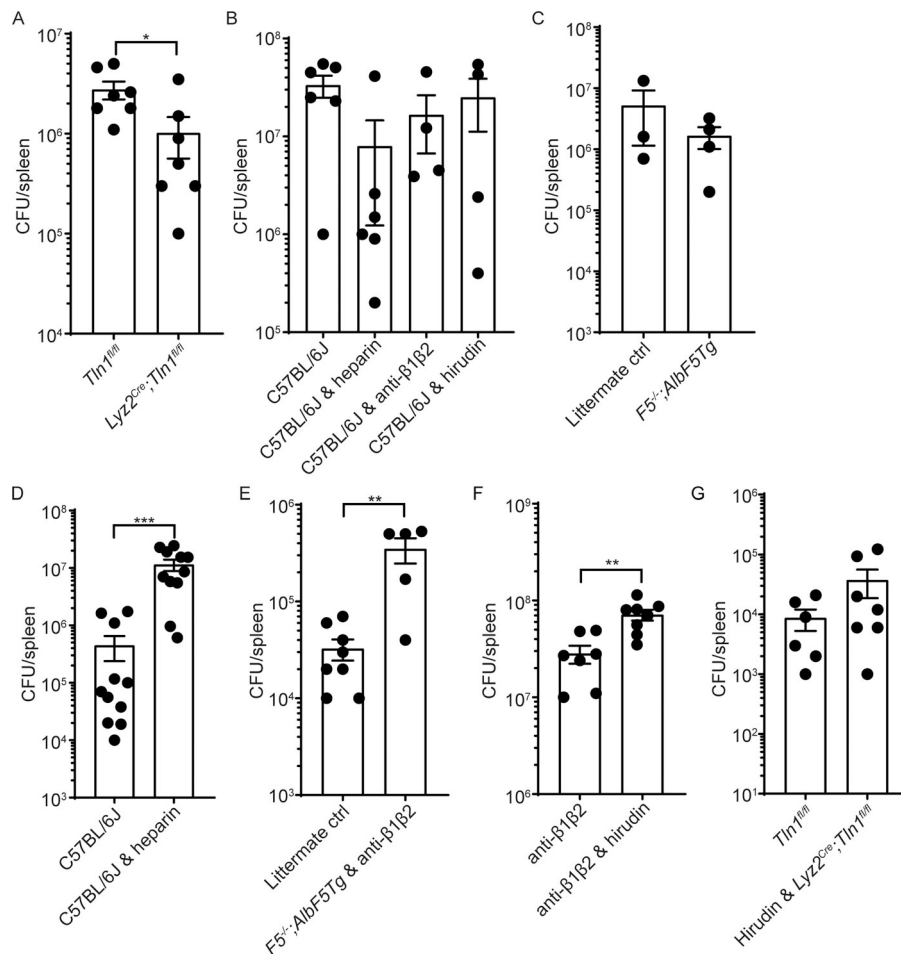
Figure 4. **MDR restricts bacterial dissemination out of the peritoneal cavity to the spleen.** **(A)** CFUs per spleen from $Tln1^{fl/fl}$ mice or $Lyz2^{Cre}$; $Tln1^{fl/fl}$ mice at 16 h after i.v. E. coli infection. **(B)** CFUs per spleen from mice untreated or treated with heparin, anti-integrin β1 and β2 blocking antibodies, or hirudin at 16 h after i.v. E. coli infection. Differences between groups are not statistically significant. **(C)** CFU per spleen from F5 littermates and $F5^{-/-}$;AlbF5Tg mice at 16 h after i.v. E. coli infection. Differences are not statistically significant. Ctrl, control. **(D)** CFUs per spleen from untreated and heparin-treated mice at 16 h after i.p. E. coli infection. **(E)** CFUs per spleen from F5 littermates and $F5^{-/-}$;AlbF5Tg mice treated with anti-integrin β1 and β2 blocking antibodies at 16 h after i.p. E. coli infection. **(F)** CFUs per spleen from mice treated with anti-integrin β1 and β2 blocking antibodies and mice treated with hirudin and anti-integrin β1 and β2 blocking antibodies at 16 h after i.p. E. coli infection. **(G)** CFUs per spleen from $Tln1^{fl/fl}$ mice or $Lyz2^{Cre}$;$Tln1^{fl/fl}$ mice treated with hirudin at 16 h after i.p. E. coli infection. Differences are not statistically significant. Two-tailed t tests were used to test statistical significance for A and C–G. One-way ANOVA was used to test statistical significance for B. Symbols represent individual mice studied. Error bars represent ± SEM. All experiments were repeated at least one to three times. *, $P < 0.05$; **, $P < 0.01$; ***, $P < 0.001$.

resident macrophage–mediated coagulation produces important beneficial effects.

Materials and methods

Mice

All C57BL/6J mice were purchased at the age of 8 wk from The Jackson Laboratory. $Lyz2^{Cre}$;$Tln1^{fl/fl}$ mice were a kind gift from Dr. Rodger P. McEver (Oklahoma Medical Research Foundation, Oklahoma City, OK). Low human TF mice, $Lyz2^{Cre}$;$F3^{fl/fl}$ mice, $F5^{-/-}$;AlbF5Tg mice, $Lyz2^{Cre}$;$Gata6^{fl/fl}$ mice (now backcrossed to C57BL/6 background), $Lyz2^{Cre}$;$R26^{LSL-Tdtomato}$ mice, and $Bhlhe40^{GFP}$ mice were described previously (Parry et al., 1998; Sun et al., 2003; Pawlinski et al., 2010; Gautier et al., 2014; Lin et al., 2016; Wang and Kubes, 2016). $Csf1r^{MeriCreMer}$;$Gata6^{fl/fl}$ mice (fully backcrossed to C57BL/6 background) were generated by crossing $Csf1r^{MeriCreMer}$ mice with $Gata6^{fl/fl}$ mice. Mouse studies were approved by animal use oversight committees at Washington University School of Medicine and the University of North Carolina (studies on TF).

Reagents

Pac Blue anti-CD45 mAb, allophycocyanin anti-ICAM2 mAb, allophycocyanin/Cy7 anti-CD11b mAb, PE anti-Ly6G mAb, PerCP/Cy5.5 anti-Ly6C mAb, PE/Cy7 anti-F4/80 mAb, and anti-ICAM2 mAb were all purchased from BioLegend. Anti-S100A9 polyclonal antibody was purchased from R&D Systems (AF2065-SP). Anti-Gata6 monoclonal antibody was purchased from Cell Signaling Technology (5851). Anti-fibrin(ogen) polyclonal antibody was purchased from Agilent Dako (A0080). The Alexa Fluor 594–conjugated heat-killed bacterial particles were purchased from Thermo Fisher Scientific (E23370). Clodronate-loaded liposome was purchased from ClodronateLiposomes.org. Recombinant hirudin was purchased from Aniara Diagnostica (ARE120A). Zymosan was purchased from Sigma-Aldrich (Z4250). GFP E. coli was purchased from ATCC (ATCC 25922GFP). Human FV–deficient plasma was purchased from Haematologic Technologies. Rabbit thromboplastin (44213), Liberase, hyaluronidase, DNase I, streptokinase, and collagenase D were purchased from Sigma-Aldrich. Plasminogen was purchased from Lee Biosolutions.

Flow cytometry

Flow cytometry was performed as described previously (Gautier et al., 2014). Briefly, peritoneal exudate cells were collected by flushing the peritoneum with 6 ml HBSS with 2.5 mM EDTA and 0.2% BSA. Peritoneal clots were collected 3 h after zymosan injection and digested using a cocktail of 1 mg/ml collagenase D, 50 U/ml streptokinase, 4 U/ml plasminogen, 100 µg/ml Liberase, 100 µg/ml DNase I, and 0.5 mg/ml hyaluronidase in RPMI with 1% FBS. The digestion was incubated at 37°C for 30 min and

mixed by pipetting every 5 min. It was then passed through 70-µm cell strainers to collect single-cell suspension for antibody staining. All antibodies were incubated with cells on ice and diluted 1:200. Peritoneal cells and clot digestions were incubated for 30 min with Pac Blue anti-CD45 mAb, allophycocyanin anti-ICAM2 mAb, allophycocyanin/Cy7 anti-CD11b mAb, PE anti-Ly6G mAb, PerCP/Cy5.5 anti-Ly6C mAb, and PE/Cy7 anti-F4/80 mAb and then washed, resuspended, and analyzed on a BD FACSCanto II (BD Biosciences) using FlowJo software.

Peritonitis models
Briefly, 1 mg zymosan or 2×10^7 E. coli ATCC 25922 was injected i.p. E. coli was washed with sterile PBS before injection. Peritoneal exudate cells, peritoneal fluid, blood, or spleens were collected at different time points after injection. The cell numbers were counted using a Nexcelom cell counter.

i.v. E. coli infection model
Briefly, 2×10^8 E. coli ATCC 25922 was injected retro-orbitally. E. coli was washed with sterile PBS before injection. Spleens were collected at 16 h after injection. CFUs were counted and calculated as below.

E. coli burden measurement
E. coli ATCC 25922 was cultured in LB medium with 100 µg/ml ampicillin overnight. CFUs were calculated based on OD_{600} and confirmed by plating the serial dilution and culturing overnight on LB plates with ampicillin. 2×10^7 E. coli was injected i.p., based on this dose as the LD_{50} from previous studies (Xiang et al., 2013). 4 h after infection, peritoneal fluid was collected, diluted accordingly, and cultured overnight on LB plates with ampicillin to count and calculate CFU on the next day. Bar graphs were plotted as CFUs per microliter of peritoneal fluid, which subsequently was used to measure TAT concentration.

Intravital two-photon microscopy
Bhlhe40^{GFP} mice were anesthetized and placed in a supine position. The abdominal skin was opened and separated from the muscle, leaving the peritoneal cavity intact. Some mice were injected with AF594-conjugated heat-killed E. coli from the left side of the peritoneal cavity (away from the imaging region) using a 30G needle while taking images. Images were collected using a customized Leica SP8 two-photon microscope equipped with a 25×, 0.95 NA water-immersion objective and a Mai Tai HP DeepSee Laser (Spectra-Physics) tuned to 900 nm. Fluorescence emission was guided directly to hybrid photodetectors. For signal separation, three dichroic beam splitters (Semrock) were used at 458, 495, and 560 nm (FF458-Di02, FF495-Di03, and FF560-Di01). Clots from GFP E. coli–infected mice were immediately placed into an imaging chamber between 50-µm mesh and a quartz coverslip to keep it at physiological temperature and was examined for up to 1 h. Most experiments focused on the 30-min time period. Clots were imaged with 20 to 35 optical sections at 2.5 µm, each taken at regular time intervals (typically 30 s), in order to capture cell dynamics within the clot.

FV activity measurement
Whole blood from C57BL/6J mice was drawn from inferior vena cava with one-tenth volume 3.8% sodium citrate. Plasma was collected by centrifuging at 2,000 g for 10 min. Peritoneal fluid was centrifuged at 5,000 g for 10 min, aliquoted, and stored in a −80°C freezer. FV activity was determined using a one-stage clotting assay with human FV–deficient plasma, as previously described, with a Coatron M1 machine. The mouse plasma was used as standard and set as 100%.

Collection of peritoneal interstitial fluid
Pure peritoneal interstitial fluid was collected as described by Hartveit and Thunold (1966). Briefly, it was collected by aspirating with a 10-µl pipette tip without any anticoagulant, centrifuged at 2,000 g for 10 min, and stored in a −80°C freezer.

Bone marrow transplantation
Bone marrow transplantation was performed as described previously (Zhang et al., 2016). Briefly, bone marrow cells were isolated from CD45.2 or $F5^{-/-}$;AlbF5Tg mice. The cells (2×10^6) were injected i.v. into lethally irradiated 6-8-wk-old CD45.1/CD45.2 mice (1,100 rad). 6 wk after transplantation, reconstitution was determined by quantitating percentages of CD45.2$^+$ resident peritoneal macrophages with flow cytometry.

TAT ELISA
TAT ELISA-paired antibodies were purchased from Cedarlane (CL20018K). The ELISA was performed as per the manufacturer's instructions. Mouse plasma was fully clotted by recalcification to generate serum that has a maximal amount of TAT. This serum was aliquoted and used as the standard. 10 µl of the peritoneal fluid was diluted 1:10 into the plate. 10 µl of the serum was diluted 1:10 and set as 100%. Bar graphs were plotted as the percentages of the serum.

Confocal microscopy
Peritoneal clots were collected 3–5 h after zymosan injection, fixed in 4% paraformaldehyde overnight at 4°C, transferred into 20% sucrose overnight at 4°C, embedded in Tissue-Tek O.C.T. Compound (Triangle Biomedical Sciences), and processed into 10-µm sections. After fixation and permeabilization in 4% paraformaldehyde for 5 min, cryosections were rinsed with PBS, incubated in PBS with 3% BSA and 1% Triton at room temperature for 60 min, and then incubated with primary antibodies (α-ICAM2, α-fibrin(ogen), α-Gata6, and α-S100A9) overnight at 4°C, washed with PBS, and incubated with secondary antibodies (Cy2, Cy3, and Cy5) at room temperature for 1 h. After washing, mounting medium was added to the slides. Images were collected using a Leica SP8 confocal microscope. Whole-mount imaging followed a similar protocol but extended antibody incubations to overnight.

Gene expression analysis
Gene expression analysis in macrophage herein used a previously described database created by the Immunological Genome Project (detailed by Gautier et al., 2014).

Statistics

Statistical analysis was performed using the Student's *t* test for unpaired samples or one-way ANOVA with a post-hoc Tukey's multiple comparisons test. Results were considered significant at $P < 0.05$. Results display all replicated experiments, and values are mean ± SEM.

Online supplemental material

Fig. S1 shows coagulation and adhesion additively cooperate to account for the MDR in response to inflammation. Video 1 shows intravital imaging of peritoneal macrophages through the intact abdominal wall. Video 2 shows intravital imaging of a clot after removal from a mouse 3 h after injection of GFP–*E. coli*.

References

Barth, M.W., J.A. Hendrzak, M.J. Melnicoff, and P.S. Morahan. 1995. Review of the macrophage disappearance reaction. *J. Leukoc. Biol.* 57:361–367. https://doi.org/10.1002/jlb.57.3.361

Bellingan, G.J., P. Xu, H. Cooksley, H. Cauldwell, A. Shock, S. Bottoms, C. Haslett, S.E. Mutsaers, and G.J. Laurent. 2002. Adhesion molecule-dependent mechanisms regulate the rate of macrophage clearance during the resolution of peritoneal inflammation. *J. Exp. Med.* 196:1515–1521. https://doi.org/10.1084/jem.20011794

Cao, C., D.A. Lawrence, D.K. Strickland, and L. Zhang. 2005. A specific role of integrin Mac-1 in accelerated macrophage efflux to the lymphatics. *Blood.* 106:3234–3241. https://doi.org/10.1182/blood-2005-03-1288

Davies, L.C., M. Rosas, S.J. Jenkins, C.T. Liao, M.J. Scurr, F. Brombacher, D.J. Fraser, J.E. Allen, S.A. Jones, and P.R. Taylor. 2013. Distinct bone marrow-derived and tissue-resident macrophage lineages proliferate at key stages during inflammation. *Nat. Commun.* 4:1886. https://doi.org/10.1038/ncomms2877

Echtenacher, B., K. Weigl, N. Lehn, and D.N. Männel. 2001. Tumor necrosis factor-dependent adhesions as a major protective mechanism early in septic peritonitis in mice. *Infect. Immun.* 69:3550–3555. https://doi.org/10.1128/IAI.69.6.3550-3555.2001

Faust, N., F. Varas, L.M. Kelly, S. Heck, and T. Graf. 2000. Insertion of enhanced green fluorescent protein into the lysozyme gene creates mice with green fluorescent granulocytes and macrophages. *Blood.* 96:719–726.

Gautier, E.L., T. Shay, J. Miller, M. Greter, C. Jakubzick, S. Ivanov, J. Helft, A. Chow, K.G. Elpek, S. Gordonov, et al; Immunological Genome Consortium. 2012. Gene-expression profiles and transcriptional regulatory pathways that underlie the identity and diversity of mouse tissue macrophages. *Nat. Immunol.* 13:1118–1128. https://doi.org/10.1038/ni.2419

Gautier, E.L., S. Ivanov, P. Lesnik, and G.J. Randolph. 2013. Local apoptosis mediates clearance of macrophages from resolving inflammation in mice. *Blood.* 122:2714–2722. https://doi.org/10.1182/blood-2013-01-478206

Gautier, E.L., S. Ivanov, J.W. Williams, S.C. Huang, G. Marcelin, K. Fairfax, P.L. Wang, J.S. Francis, P. Leone, D.B. Wilson, et al 2014. Gata6 regulates aspartoacylase expression in resident peritoneal macrophages and controls their survival. *J. Exp. Med.* 211:1525–1531. https://doi.org/10.1084/jem.20140570

Ginhoux, F., and M. Guilliams. 2016. Tissue-Resident Macrophage Ontogeny and Homeostasis. *Immunity.* 44:439–449. https://doi.org/10.1016/j.immuni.2016.02.024

Guilliams, M., and C.L. Scott. 2017. Does niche competition determine the origin of tissue-resident macrophages? *Nat. Rev. Immunol.* 17:451–460. https://doi.org/10.1038/nri.2017.42

Hartveit, F., and S. Thunold. 1966. Peritoneal fluid volume and the oestrus cycle in mice. *Nature.* 210:1123–1125. https://doi.org/10.1038/2101123a0

Lim, T.J.F., and I.H. Su. 2018. Talin1 Methylation Is Required for Neutrophil Infiltration and Lipopolysaccharide-Induced Lethality. *J. Immunol.* 201:3651–3661. https://doi.org/10.4049/jimmunol.1800567

Lin, C.C., T.R. Bradstreet, E.A. Schwarzkopf, N.N. Jarjour, C. Chou, A.S. Archambault, J. Sim, B.H. Zinselmeyer, J.A. Carrero, G.F. Wu, et al 2016. IL-1-induced Bhlhe40 identifies pathogenic T helper cells in a model of autoimmune neuroinflammation. *J. Exp. Med.* 213:251–271. https://doi.org/10.1084/jem.20150568

Meza-Perez, S., and T.D. Randall. 2017. Immunological Functions of the Omentum. *Trends Immunol.* 38:526–536. https://doi.org/10.1016/j.it.2017.03.002

Michel, C.C., M.N. Nanjee, W.L. Olszewski, and N.E. Miller. 2015. LDL and HDL transfer rates across peripheral microvascular endothelium agree with those predicted for passive ultrafiltration in humans. *J. Lipid Res.* 56:122–128. https://doi.org/10.1194/jlr.M055053

Misharin, A.V., L. Morales-Nebreda, P.A. Reyfman, C.M. Cuda, J.M. Walter, A.C. McQuattie-Pimentel, C.I. Chen, K.R. Anekalla, N. Joshi, K.J.N. Williams, et al 2017. Monocyte-derived alveolar macrophages drive lung fibrosis and persist in the lung over the life span. *J. Exp. Med.* 214:2387–2404. https://doi.org/10.1084/jem.20162152

Nelson, D.S. 1963. Reaction to antigens in vivo of the peritoneal macrophages of guinea-pigs with delayed type hypersensitivity. Effects of anti-coagulants and other drugs. *Lancet.* 2:175–176. https://doi.org/10.1016/S0140-6736(63)92808-3

Okabe, Y., and R. Medzhitov. 2014. Tissue-specific signals control reversible program of localization and functional polarization of macrophages. *Cell.* 157:832–844. https://doi.org/10.1016/j.cell.2014.04.016

Osterud, B., J. Bögwald, U. Lindahl, and R. Seljelid. 1981. Production of blood coagulation factor V and tissue thromboplastin by macrophages in vitro. *FEBS Lett.* 127:154–160. https://doi.org/10.1016/0014-5793(81)80363-8

Parry, G.C., J.H. Erlich, P. Carmeliet, T. Luther, and N. Mackman. 1998. Low levels of tissue factor are compatible with development and hemostasis in mice. *J. Clin. Invest.* 101:560–569. https://doi.org/10.1172/JCI814

Pawlinski, R., J.G. Wang, A.P. Owens III, J. Williams, S. Antoniak, M. Tencati, T. Luther, J.W. Rowley, E.N. Low, A.S. Weyrich, and N. Mackman. 2010. Hematopoietic and nonhematopoietic cell tissue factor activates the coagulation cascade in endotoxemic mice. *Blood.* 116:806–814. https://doi.org/10.1182/blood-2009-12-259267

Pejler, G., C. Lunderius, and B. Tomasini-Johansson. 2000. Macrophages synthesize factor X and secrete factor X/Xa-containing prothrombinase

activity into the surrounding medium. *Thromb. Haemost.* 84:429–435. https://doi.org/10.1055/s-0037-1614040

Rosas, M., L.C. Davies, P.J. Giles, C.T. Liao, B. Kharfan, T.C. Stone, V.B. O'Donnell, D.J. Fraser, S.A. Jones, and P.R. Taylor. 2014. The transcription factor Gata6 links tissue macrophage phenotype and proliferative renewal. *Science.* 344:645–648. https://doi.org/10.1126/science.1251414

Sun, H., T.L. Yang, A. Yang, X. Wang, and D. Ginsburg. 2003. The murine platelet and plasma factor V pools are biosynthetically distinct and sufficient for minimal hemostasis. *Blood.* 102:2856–2861. https://doi.org/10.1182/blood-2003-04-1225

Szaba, F.M., and S.T. Smiley. 2002. Roles for thrombin and fibrin(ogen) in cytokine/chemokine production and macrophage adhesion in vivo. *Blood.* 99:1053–1059. https://doi.org/10.1182/blood.V99.3.1053

Wang, J., and P. Kubes. 2016. A Reservoir of Mature Cavity Macrophages that Can Rapidly Invade Visceral Organs to Affect Tissue Repair. *Cell.* 165:668–678. https://doi.org/10.1016/j.cell.2016.03.009

Woods, A., J.R. Couchman, S. Johansson, and M. Höök. 1986. Adhesion and cytoskeletal organisation of fibroblasts in response to fibronectin fragments. *EMBO J.* 5:665–670. https://doi.org/10.1002/j.1460-2075.1986.tb04265.x

Xiang, B., G. Zhang, L. Guo, X.A. Li, A.J. Morris, A. Daugherty, S.W. Whiteheart, S.S. Smyth, and Z. Li. 2013. Platelets protect from septic shock by inhibiting macrophage-dependent inflammation via the cyclooxygenase 1 signalling pathway. *Nat. Commun.* 4:2657. https://doi.org/10.1038/ncomms3657

Yago, T., B.G. Petrich, N. Zhang, Z. Liu, B. Shao, M.H. Ginsberg, and R.P. McEver. 2015. Blocking neutrophil integrin activation prevents ischemia-reperfusion injury. *J. Exp. Med.* 212:1267–1281. https://doi.org/10.1084/jem.20142358

Yang, T.L., J. Cui, A. Rehumtulla, A. Yang, M. Moussalli, R.J. Kaufman, and D. Ginsburg. 1998. The structure and function of murine factor V and its inactivation by protein C. *Blood.* 91:4593–4599.

Zhang, N., Z. Liu, L. Yao, P. Mehta-D'souza, and R.P. McEver. 2016. P-Selectin Expressed by a Human SELP Transgene Is Atherogenic in Apolipoprotein E-Deficient Mice. *Arterioscler. Thromb. Vasc. Biol.* 36:1114–1121. https://doi.org/10.1161/ATVBAHA.116.307437